JOURNAL OF GUIDANCE, CONTROL, AND DYNAMICS
Vol. 25, No. 5, September–October 2002

Robust Control System Design for Rotorcraft

Chih-Min Lin and Chen-Ling Ying
Yuan-Ze University, Tao-Yuan 320, Taiwan, Republic of China

A design method is developed for quantitative robust control of uncertain multivariable systems. This method is then applied for the longitudinal flight control of a rotorcraft. A multivariable equivalent external disturbance rejection design method is introduced. When this method is used, the maximum variations of the system tolerance and the maximum variations of the uncertain plant can be transferred to an equivalent disturbance. This equivalent external disturbance rejection design method is employed to achieve the quantitative robust performance for uncertain multivariable systems. The design method is then applied to the robust control design of a rotorcraft flight control system with various flight conditions and shows that it achieves satisfactory robust performance.

Nomenclature

B_h = universal high-frequency bound
$\dot{h}$ = z-body axis component of vehicle velocity, ft/s
$\dot{h}_C$ = command of z-body axis component of vehicle velocity, ft/s
δ_B = longitudinal cycle input, in. in cockpit
δ_C = main rotor collective input, in. in cockpit
θ = vehicle pitch attitude, rad
θ_C = command value of pitch attitude, rad

I. Introduction

ROTORCRAFT flight control systems present significant design challenges. Large variations in the response characteristics of rotorcraft result from the wide range of airspeeds of typical operation, varying from hover to over 100 kn. Also, the rotor degrees of freedom can have a significant impact on the system performance and stability. The main purpose of intentionally using feedback structure is to improve the tracking performance.

Recent control design research has concentrated on the development of control systems that are robust to plant variations and parametric uncertainties. Quantitative feedback theory (QFT) is an effective design method for plants with significant uncertainties.[1–4] Traditional QFT studies manipulated plant templates (sets of complex numbers due to plant parameter variations for each frequency) on a Nichols chart to obtain the bounds at some perturbed frequencies (see Refs. 1–4). Previously, several multi-input/multi-output (MIMO) QFT design methods have been proposed,[5–9] and the rotorcraft flight control system design has been presented using the traditional QFT design technique.[10–12] However, beginning the design procedure, one must first calculate and construct the plant templates, and then move them on the Nichols chart to get the uncertain bounds. This is a time-consuming design procedure. Moreover, the inverse matrix of the whole plant family is required for the design procedure. Thus, the MIMO QFT design is complicated and tedious, even for a control engineer with QFT design experience. Recently, several variants of QFT have been proposed to simplify the design procedure. One attractive design method is the equivalent external disturbance rejection (EEDR) method, which can avoid the troublesome template manipulation as the tranditional QFT does.[13–15] However, the EEDR design method is restricted to single-input/single-output systems in Refs. 13–15. The EEDR design method for MIMO systems has been proposed in Ref. 16; however, it is only applicable to minimum-phase systems.

In this paper, a multivariable EEDR design method is introduced with the capability of handling stable or unstable, minimum or nonminimum phase systems. Using this EEDR method, the maximum variations of the system tolerance and the maximum variations of the uncertain plant can be transferred to an external disturbance. By such a transformation, the templates are no longer needed. The bounds

Chih-Min Lin received B.S. and M.S. degrees in control engineering and a Ph.D. degree in electronics engineering from National Chiao Tung University, Taiwan, Republic of China, in 1981, 1983, and 1986, respectively. During 1986–1992, he was with the Chung Shan Institute of Science and Technology as a Deputy Director of System Engineering of a missile system. He also served concurrently as an Associate Professor at Chiao Tung University and Chung Yuan University, Taiwan, Republic of China. He joined the faculty of the Department of Electrical Engineering, Yuan-Ze University, Chung-Li, Taiwan, Republic of China in 1993 and is currently a Professor of Electrical Engineering. He also served as the Committee Member of Chinese Automatic Control Society and the Deputy Chairman of the IEEE Control Systems Society, Taipei Section. During 1997–1998, he was the honor research fellow in the University of Auckland, New Zealand. His research interests include guidance and flight control, intelligent control, and systems engineering. E-mail: cml@ee.yzu.edu.tw.

Chen-Ling Ying received M.S. degrees in electrical engineering from Yuan-Ze University, Chung-Li, Taiwan, Republic of China, in 1995. Currently he is working toward a Ph.D degree in electrical engineering at the same university. His research interests include robust control, optimal control, and flight control systems.

Received 10 December 2001; revision received 11 May 2002; accepted for publication 15 May 2002.

are calculated algebraically and are obtained easily on the inverse Nichols chart, instead of manipulating templates on the Nichols chart. Thus the design procedures of EEDR are easier than the traditional QFT design methods, especially in MIMO systems. This paper also investigates the feasibility of utilizing EEDR designed for a longitudinal channel robust control of a rotorcraft that meets flying tolerance within the flight envelope. A BO105C rotorcraft is utilized as the design example to illustrate the effectiveness of the proposed design method.

II. Robust Feedback Controller Design

The quantitative robust performance design objective is to find the controllers to guarantee that the system performance bounds are satisfied over the range of plant uncertainties. Because the robust control design procedures are in the frequency domain, the performance bounds are given in the frequency domain:

$$B_l(s) \le T(s) \le B_u(s) \tag{1}$$

where $T(s)$ is the closed-loop transfer function and $B_l(s)$ and $B_u(s)$ are its lower and upper bounds, respectively.

Consider a MIMO two-degree-of-freedom (2-DOF) feedback system, as shown in Fig. 1, where $\boldsymbol{P}_0(s) = [p_{oij}]$, $\boldsymbol{P}(s) = [p_{ij}]$, $\boldsymbol{G}(s) = [g_{ij}]$, and $\boldsymbol{F}(s) = [f_{ij}] \in \boldsymbol{C}^{n\times n}$ are the nominal plant, uncertain plant, feedback controller, and prefilter, respectively. Let $\boldsymbol{T} = [t_{ij}]$ and $\boldsymbol{T}_0 = [t_{oij}]$ be the perturbed and nominal system transfer matrices from r to y, respectively, and define $\Delta\boldsymbol{T} = \boldsymbol{T} - \boldsymbol{T}_0$ and $\boldsymbol{L}_0 = [l_{oij}] = \boldsymbol{P}_0\boldsymbol{G}$. Assume that $\boldsymbol{P}$ and $(\boldsymbol{I} + \boldsymbol{L}_0)$ are nonsingular matrices, and define $\boldsymbol{P}_v = [v_{ij}] = \boldsymbol{I} - \boldsymbol{P}_0\boldsymbol{P}^{-1}$ and $\boldsymbol{T}_v = \boldsymbol{I} - \boldsymbol{T}_0\boldsymbol{T}^{-1}$. Then the following theorem can be obtained.

Theorem 1: Consider a MIMO, 2-DOF system as shown in Fig. 1, where the relation between $\boldsymbol{T}_v$ and $\boldsymbol{P}_v$ can be expressed as follows:

$$\boldsymbol{T}_v = (\boldsymbol{I} + \boldsymbol{L}_0)^{-1}\boldsymbol{P}_v \tag{2}$$

Proof: From Fig. 1, the following is obtained:

$$y = \boldsymbol{P}(\boldsymbol{F}r - \boldsymbol{G}y) \tag{3}$$

and then

$$(\boldsymbol{I} + \boldsymbol{P}\boldsymbol{G})y = \boldsymbol{P}\boldsymbol{F}r \tag{4}$$

From Eq. (4), the following is obtained:

$$(\boldsymbol{P}^{-1} + \boldsymbol{G})y = \boldsymbol{F}r \tag{5}$$

then

$$\left(\boldsymbol{P}_0\boldsymbol{P}^{-1} + \boldsymbol{P}_0\boldsymbol{G}\right)y = \boldsymbol{P}_0\boldsymbol{F}r \tag{6}$$

that is,

$$\left(\boldsymbol{P}_0\boldsymbol{P}^{-1} + \boldsymbol{L}_0\right)\boldsymbol{T} = \boldsymbol{P}_0\boldsymbol{F} \tag{7}$$

Equation (7) can be rewritten as

$$(\boldsymbol{I} + \boldsymbol{L}_0)\boldsymbol{T} = \boldsymbol{P}_0\boldsymbol{F} + \boldsymbol{P}_v\boldsymbol{T} \tag{8}$$

Because the nominal system transfer matrix is

$$\boldsymbol{T}_0 = (\boldsymbol{I} + \boldsymbol{L}_0)^{-1}\boldsymbol{P}_0\boldsymbol{F} \tag{9}$$

then Eq. (9) becomes

$$(\boldsymbol{I} + \boldsymbol{L}_0)(\boldsymbol{T} - \boldsymbol{T}_0) = \boldsymbol{P}_v\boldsymbol{T} \tag{10}$$

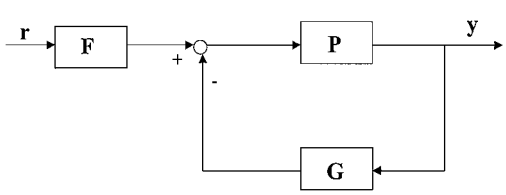

Fig. 1 Feedback control system with 2 DOF.

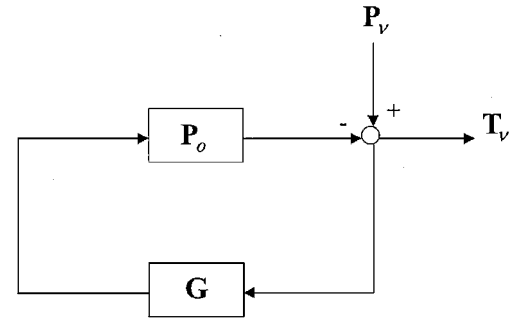

Fig. 2 Equivalent external disturbance system.

Because $(\boldsymbol{I} + \boldsymbol{L}_0)^{-1}$ exists, Eq. (10) can be rewritten as

$$\Delta\boldsymbol{T} \equiv \boldsymbol{T} - \boldsymbol{T}_0 = (\boldsymbol{I} + \boldsymbol{L}_0)^{-1}\boldsymbol{P}_v\boldsymbol{T} \tag{11}$$

that is,

$$\boldsymbol{T}_v = (\boldsymbol{I} + \boldsymbol{L}_0)^{-1}\boldsymbol{P}_v \tag{12}$$

□

As the result, the feedback-loop block diagram in Fig. 1 can also be redrawn as Fig. 2. The uncertainty of $\boldsymbol{P}$ is transferred to the equivalent disturbance term $\boldsymbol{P}_v$ and the tolerance of the system response is transferred to the system output term $\boldsymbol{T}_v$.

The physical meaning of the relation between Figs. 1 and 2 is described as follows. Fix the parameters of $\boldsymbol{P}$ and use an additional external disturbance $\boldsymbol{P}_v$ to simulate the effect of the variations of the plant parameters. Thus, the rejection of the external disturbance $\boldsymbol{P}_v$ is similar to coping with the parameter variations of $\boldsymbol{P}$. Figure 2 also shows that the loop transfer function matrix $\boldsymbol{L}_0 = \boldsymbol{P}_0\boldsymbol{G}$ is designed to reduce the sensitivity, with respect to the equivalent disturbance $\boldsymbol{P}_v$.

A. Derivation of the Variation Bounds

For a MIMO system, Eq. (2) can be expressed as

$$\Delta t_{ij} = \frac{v_{ii}t_{ij} + \sum_{k=1,k\neq i}^{n}(v_{ik}t_{kj} - l_{ik}\Delta t_{kj})}{1 + l_{oii}} \qquad i, j = 1, 2, \ldots, n \tag{13}$$

then the design equations are derived as follows.

For $i = j$, Eq. (13) can be rewritten as

$$\frac{1}{1 + l_{oii}} = \frac{\Delta t_{ii}/t_{ii}}{v_{ii} + \sum_{k=1,k\neq i}^{n}(v_{ik}t_{ki} - l_{ik}\Delta t_{ki})/t_{ii}} \tag{14}$$

and the logarithmic expression of Eq. (14) can be written as

$$\left|\frac{1}{1 + l_{oii}}\right|_{\mathrm{dB}} = \left|\frac{\Delta t_{ii}}{t_{ii}}\right|_{\mathrm{dB}} - \left|v_{ii} + \sum_{k=1,k\neq i}^{n}\frac{v_{ik}t_{ki} - l_{ik}\Delta t_{ki}}{t_{ii}}\right|_{\mathrm{dB}}$$
$$= |t_{dii}|_{\mathrm{dB}} - |p_{dii}|_{\mathrm{dB}} \tag{15}$$

where $t_{dii} = \Delta t_{ii}/t_{ii}$ and

$$p_{dii} = v_{ii} + \sum_{k=1,k\neq i}^{n}\frac{(v_{ik}t_{ki} - l_{ik}\Delta t_{ki})}{t_{ii}}$$

Similarly, for $i \neq j$, Eq. (13) can be expressed as

$$\frac{1}{1 + l_{oii}} = \frac{\Delta t_{ij}/t_{ij}}{v_{ii} + \sum_{k=1,k\neq i}^{n}(v_{ik}t_{kj} - l_{ik}\Delta t_{kj})/t_{ij}} \tag{16}$$

and the logarithmic expression is shown as

$$\left|\frac{1}{1 + l_{oii}}\right|_{\mathrm{dB}} = \left|\frac{\Delta t_{ij}}{t_{ij}}\right|_{\mathrm{dB}} - \left|v_{ii} + \sum_{k=1,k\neq i}^{n}\frac{v_{ik}t_{kj} - l_{ik}\Delta t_{kj}}{t_{ij}}\right|_{\mathrm{dB}}$$
$$= |t_{dij}|_{\mathrm{dB}} - |p_{dij}|_{\mathrm{dB}} \tag{17}$$

where $t_{dij} = \Delta t_{ij}/t_{ij}$ and

$$p_{dij} = v_{ii} + \sum_{k=1,k\neq i}^{n} \frac{(v_{ik}t_{kj} - l_{ik}\Delta t_{kj})}{t_{ij}}$$

Therefore, the nominal-loop transmission function l_{oii} should be designed to satisfy

$$|1/(1+l_{oii})|_{\mathrm{dB}} \leq \min(|t_{dii}|_{\mathrm{dB}} - |p_{dii}|_{\mathrm{dB\,max}}, |t_{dij}|_{\mathrm{dB}} - |p_{dij}|_{\mathrm{dB\,max}}) \tag{18}$$

In the calculation of p_{dii} and p_{dij}, the term $l_{ik}\Delta t_{kj}$ can be set to zero to simplify calculations. This term can be considered as the MIMO interactions, which can be included in the coupling performance specification. For specified frequencies, the value in the right-hand part of inequality (18) is the bound $B_{oi}(\omega)$ of $l_{oii}(s)$. Then a proper loop transmission function $l_{oii}(s)$ can be obtained on the inverse Nichols chart.

After loop shaping, the nominal-loop transmission function $l_{oii}(s)$ can be obtained to satisfy the system response tolerance. Then the feedback controller can be determined as

$$\boldsymbol{G}(s) = \mathrm{diag}[g_{ii}(s)] \tag{19}$$

where

$$g_{ii}(s) = l_{oii}(s)/p_{oii}(s), \qquad i = 1, 2, \ldots, n \tag{20}$$

B. Nonminimum Phase Design

In control system design, p_{ii} the nonminimum phase (NMP) property is evidenced by the presence of right-half-plane (RHP) zeros, which limit the benefits of feedback. Suppose the uncertain plant transfer function has one or more zeros in RHP, let

$$p_{ii}(s) = N_i(-s)p_{mii}(s), \qquad i = 1, 2, \ldots, n \tag{21}$$

where

$$N_i(-s) = \prod_k (1 - \tau_k s), \qquad \tau_k > 0$$

where $-s$ is used to emphasize its RHP character and $p_{mii}(s)$ is the stable part of $p_{ii}(s)$. Let $N_{oi}(-s)$ be the nominal value of $N_i(-s)$. Then, the loop transmission function $l_{ii}(s)$ and the nominal loop transmission function $l_{oii}(s)$ can be expressed as

$$l_{ii}(s) = p_{ii}(s)g_{ii}(s) = \left[\frac{N_i(-s)}{N_i(s)}\right] \cdot [N_i(s)p_{mii}(s)g_{ii}(s)]$$

$$= A_i(s)l_{mii}(s) \tag{22}$$

$$l_{oii}(s) = p_{oii}(s)g_{ii}(s) = \left[\frac{N_{oi}(-s)}{N_{oi}(s)}\right] \cdot [N_{oi}(s)p_{moii}(s)g_{ii}(s)]$$

$$= A_{oi}(s)l_{moii}(s) \tag{23}$$

where $A_i(s) = N_i(-s)/N_i(s)$ and $A_{oi}(s) = N_{oi}(-s)/N_{oi}(s)$ are the perturbed and nominal all-pass filters, respectively, and $l_{mii}(s) = N_i(s)p_{mii}(s)g_{ii}(s)$ and $l_{moii}(s) = N_{oi}(s)p_{moii}(s)g_{ii}(s)$ are the perturbed and nominal loop-transmission functions without RHP zeros, respectively. Because $|A_{oi}(s)| = 1$, it is revealed that

$$|l_{moii}(s)| = |l_{oii}(s)| \tag{24}$$

$$\angle l_{moii}(s) = \angle l_{oii}(s) - \angle A_{oi}(s) \tag{25}$$

that is, when a comparison is made between an NMP and a minimum-phase system, both of their magnitudes are the same, but $l_{oii}(s)$ has more phase lag because of $A_{oi}(s)$. Thus the bounds' relationships between minimum-phase system and NMP system are described as

$$B_{oi}(s) = A_{oi}(s)B_{moi}(s) \tag{26}$$

Therefore, the EEDR design can be extended to NMP by applying Eqs. (24) and (25). Once the values of $|l_{moii}(s)|$ can be found, the bounds B_{moi} of l_{moii} can be obtained using Eq. (15), Eq. (17), and inequality (18). Then, from Eq. (26), the bounds $B_{oi}(\omega)$ of l_{oii} with NMP can be obtained.

Remark: In Ref. 16, the loop transfer matrix $\boldsymbol{L}_0 = \boldsymbol{P}_0\boldsymbol{G}$ is taken as diagonal. Because $\boldsymbol{L}_0$ has been shaping, then the controller $\boldsymbol{G}$ is calculated by $\boldsymbol{G} = \boldsymbol{P}_0^{-1}\boldsymbol{L}_0$. This will easily result in unstable pole-zero cancellation when the plant $\boldsymbol{P}$ contains any RHP zero, so that in Ref. 16, it is only applicable for minimum-phase systems. However, in the design method proposed here, $\boldsymbol{G}$ is taken to be diagonal as in Eq. (19), where $g_{ii}(s)$ is determined from Eq. (20). The RHP zero problem of $p_{ii}(s)$ can be solved as discussed in earlier in this section.

From the preceding analysis, the following EEDR design algorithm for MIMO control systems is presented:

1) Choose the nominal and perturbed plant and closed-loop transfer functions, $p_{oii}(s)$, $t_{oii}(s)$, $p_{ii}(s)$, $t_{ii}(s)$, and let $t_{oij} = 0$.

a) For the plants, choose the minimum (maximum) values of the parameter variation intervals as the nominal plant and the maximum (minimum) one as perturbed plant.

b) For the closed-loop transfer functions, choose the lower (upper) transfer function of the system specifications as $t_{oii}(s)$ and upper (lower) one as $t_{ii}(s)$.

2) Define the coupling specifications $|t_{ij}/t_{ii}|$ and find the bounds $B_{oi}(s)$ of $l_{oii}(s)$ for minimum-phase $p_{ii}(s)$ and bounds $B_{moii}(s)$ of $l_{moii}(s)$ for NMP $p_{ii}(s)$ from Eq. (15), Eq. (17), and inequality (18). At high frequency, the plant

$$p_{ii}(s) = k\prod(s + z_i)\Big/\prod(s + p_i)$$

degenerates into ks^{-e}, where e is the excess of poles of p_{ii} over zeros of p_{ii}. The plant variation approaches a vertical line of length $|k_{\max}/k_o|$, where $k_{\max}$ and k_o are the maximum and nominal values of k, respectively. Hence, with the disturbance response constraint, one could construct an universal high-frequency bound B_h (Ref. 13).

3) Shape the nominal-loop transmission function. At each specified frequency, $l_{oii}(s)$ [or $l_{moii}(s)$] must be on or above or outside around the specified frequency bound of step 2. Then from Eqs. (19) and (20), the feedback controller $\boldsymbol{G}(s)$ can be determined. Finally, shape the prefilter $\boldsymbol{F}(s) = \mathrm{diag}[f_{ii}(s)]$ to confirm that the closed-loop transfer functions are located in the specified bounds.

III. Illustrative Example

The BO105C rotorcraft system is considered as the design example, and the system dynamic equations for different flight conditions are given in Ref. 11. The rotorcraft system involves the longitudinal control for an airspeed range from 0 to 100 kn. It is assumed that an attitude command system in pitch and a rate command system in vertical translation are desired. Thus, the attitude command θ_c and the vertical translation rate command $\dot{h}_c$ are assumed to be generated by the pilot through cockpit control deflections. The BO105C rotorcraft dynamics equations for different flight conditions are given in Tables 1 and 2, where $(a) = (s + a)$ and $[\xi; \omega] = (s^2 + 2\xi\omega s + \omega^2)$. Also note the unstable and NMP dynamics of $p_{ii}(s)$ appearing in Tables 1 and 2. These data were derived assuming very tight control of the lateral–directional axes, that is, it was done using coupling numerators to create the longitudinal dynamics under the assumption of tightly controlled lateral–directional modes.[17]

1) The flight condition at 20 kn is chosen as the nominal plant, and the flight condition at 100 kn is chosen as the perturbed one. Define the coupling specifications as

$$|t_{12}/t_{22}| \leq 0.2 \tag{27}$$

$$|t_{21}/t_{11}| \leq 0.3 \tag{28}$$

2) The bounds of the desired performance specifications are chosen as follows.

Lower bound of $\dot{h}$:

$$B_{1l} = \dot{h}/\dot{h}_c = 1/(s/2 + 1)[(s/5.5)^2 + 2(0.78/5.5)s + 1] \tag{29}$$

Upper bound of $\dot{h}$:

$$B_{1u} = \dot{h}/\dot{h}_c = 1/[(s/4.5)^2 + 2(1/4.5)s + 1] \tag{30}$$

Table 1 BO105C dynamic equations for different flight conditions

Airspeed, kn	$\dot{h}/\delta_C$, ft/s · in.	$\dot{h}/\delta_B$, ft/s · in.
0	$\frac{-9.89(0.00363)(3.6)[-0.0572;\ 0.433]}{(0.00264)(0.333)(3.6)[-0.053;\ 0.433]}$	$\frac{-0.384(0)[0.0608;\ 0.605]}{(0.00264)(0.333)(3.6)[-0.053;\ 0.433]}$
20	$\frac{-9.4(0.0363)(3.66)[-0.0353;\ 0.429]}{(0.0351)(0.45)(3.69)[-0.0472;\ 0.44]}$	$\frac{0.474(0.035)(-0.399)[0.314;\ 5.82]}{(0.0351)(0.45)(3.69)[-0.0472;\ 0.44]}$
40	$\frac{-10.2(0.0356)(3.61)[-0.0706;\ 0.425]}{(0.0348)(0.5199)(3.92)[-0.115;\ 0.476]}$	$\frac{1.06(0.0351)(-0.0747)[0.296;\ 6.48]}{(0.0348)(0.5199)(3.92)[-0.115;\ 0.476]}$
60	$\frac{-11.42(0.0470)(3.21)[-0.746;\ 0.423]}{(0.0463)(0.474)(4.54)[-0.182;\ 0.456]}$	$\frac{1.73(0.0089)(0.0472)[0.281;\ 6.8]}{(0.0463)(0.474)(4.54)[-0.182;\ 0.456]}$
80	$\frac{-12.7(0.0603)(0.162)[-0.923;\ 0.2.02]}{(0.0598)(0.474)(4.54)[-0.308;\ 0.456]}$	$\frac{2.47(0.0392)(0.0617)[0.285;\ 6.96]}{(0.0598)(0.474)(4.54)[-0.308;\ 0.456]}$
100	$\frac{-13.8(0.0751)(0.148)[-0.729;\ 0.2.55]}{(0.0747)(0.421)(4.94)[-0.563;\ 0.531]}$	$\frac{3.25(0.0565)(0.0780)[0.287;\ 7.07]}{(0.0747)(0.421)(4.94)[-0.563;\ 0.531]}$

Table 2 BO105C dynamic equations for different flight conditions

Airspeed, kn	θ/δ_c rad/in.	θ/δ_B rad/in.
0	$\frac{-0.121(0.0072)(-0.0274)(0.118)}{(0.00264)(0.333)(3.6)[-0.053;\ 0.433]}$	$\frac{-1(0)(0.0025)(0.332)}{(0.00264)(0.333)(3.6)[-0.053;\ 0.433]}$
20	$\frac{0.0467(0.033)(-0.0805)(0.286)}{(0.0351)(0.45)(3.69)[-0.0472;\ 0.44]}$	$\frac{-1(0.46)(0.0077)(0.0351)}{(0.0351)(0.45)(3.69)[-0.0472;\ 0.44]}$
40	$\frac{0.239(-0.0168)(0.0314)(0.256)}{(0.0348)(0.5199)(3.92)[-0.115;\ 0.476]}$	$\frac{-1(0.0127)(0.035)(0.647)}{(0.0348)(0.5199)(3.92)[-0.115;\ 0.476]}$
60	$\frac{0.51(0.022)(0.045)(0.483)}{(0.0463)(0.474)(4.54)[-0.182;\ .456]}$	$\frac{-1.03(0.0222)(0.0465)(0.761)}{(0.0463)(0.474)(4.54)[-0.182;\ 0.456]}$
80	$\frac{0.765(0.319)(0.595)(0.574)}{(0.0598)(0.474)(4.54)[-0.308;\ 0.456]}$	$\frac{-1.08(0.0304)(0.0601)(0.828)}{(0.0598)(0.474)(4.54)[-0.308;\ 0.456]}$
100	$\frac{1(0.037)(0.0746)(0.590)}{(0.0747)(0.421)(4.94)[-0.563;\ 0.531]}$	$\frac{-1.13(0.0364)(0.0750)(0.867)}{(0.0747)(0.421)(4.94)[-0.563;\ 0.531]}$

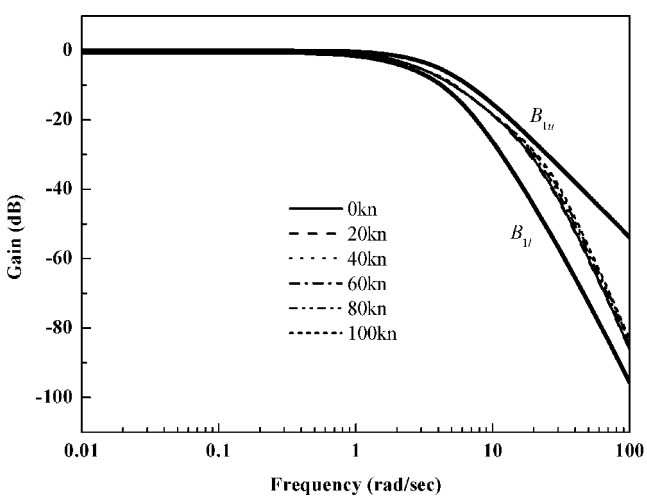

Fig. 3a Closed-loop system frequency responses $\dot{h}/\dot{h}_c$: bounds and responses for six flight conditions.

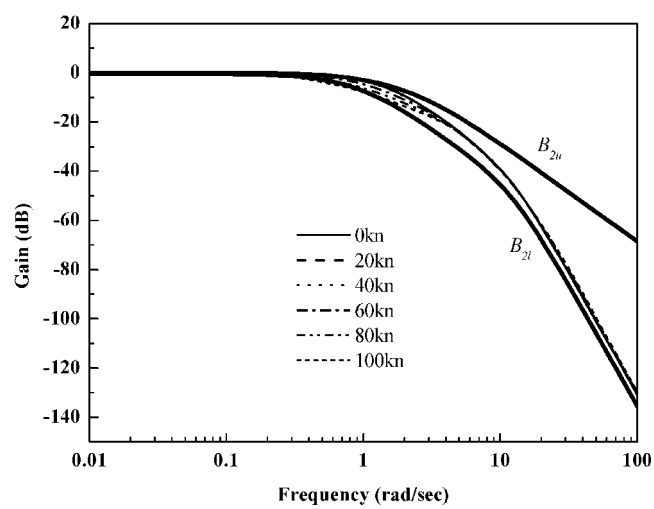

Fig. 3b Closed-loop system frequency responses θ/θ_c: bounds and responses for six flight conditions.

Lower bound of θ:

$$B_{2l} = \theta/\theta_c = 1/(s/25+1)([(s/0.9)^2 + 2(1/0.9)s + 1])([(s/12)^2 + 2(0.707/12)s + 1]) \quad (31)$$

Upper bound θ:

$$B_{2u} = \frac{\theta}{\theta_c} = \frac{(1/1.5s+1)}{(s+1)(1/2s+1)(1/2.8s+1)} \quad (32)$$

3) The feedback controller and prefilter design are the last step.

For channel 1, B_{1l} and B_{1u} are chosen as nominal and perturbed system responses, as shown in Fig. 3a. The process and the values of bounds are shown in Table 3 and Fig. 4a. After loop shaping, the nominal-loop transmission function is chosen as

$$l_{mo11}(s) = \frac{44{,}550(s+1)(s^2+0.0302s+0.1840)}{s(s+0.1)(s+45)(s+75)(s^2+0.0415s+0.1936)} \quad (33)$$

and then the required controller $g_{11}(s)$ is obtained as

$$g_{11}(s) = \frac{-4739.3617(s+0.0315)(s+0.45)(s+1)(s+3.69)}{s(s+0.0363)(s+0.1)(s+3.66)(s+45)(s+75)} \quad (34)$$

By the use of simple shaping, the prefilter is obtained as

Table 3 Bounds calculating of loop transmission $l_{mo11}(s)$ for BO105C

ω	$\lvert t_{d11}\rvert_{\text{dB}} - \lvert p_{d11}\rvert_{\text{dB max}}$	$\lvert t_{d12}\rvert_{\text{dB}} - \lvert p_{d12}\rvert_{\text{dB max}}$	$\lvert 1/1 + l_{o11}\rvert_{\text{dB}}$	Phase shift
0.6	−23.8080	−20.3202	−23.8080	−5.2429
1	−17.8554	−14.0981	−17.8554	−1.6456
5	−1.9415	1.3788	−1.9415	−0.2600
10	−0.9908	2.1745	−0.9908	−0.1292

Table 4 Bounds calculating of loop transmission $l_{mo22}(s)$ for BO105C

ω	$\lvert t_{d22}\rvert_{\text{dB}} - p_{d22}\rvert_{\text{dB max}}$	$t_{d21}\rvert_{\text{dB}} - p_{d21}\rvert_{\text{dB max}}$	$\lvert 1/1 + l_{o22}\rvert_{\text{dB}}$	Phase shift
0.6	−18.7097	−18.2264	−18.7097	−17.0356
1	−9.4190	−8.7685	−9.4190	−5.8971
5	7.4004	9.4697	7.4004	−0.9593
10	13.4573	15.8951	13.4573	−0.4768

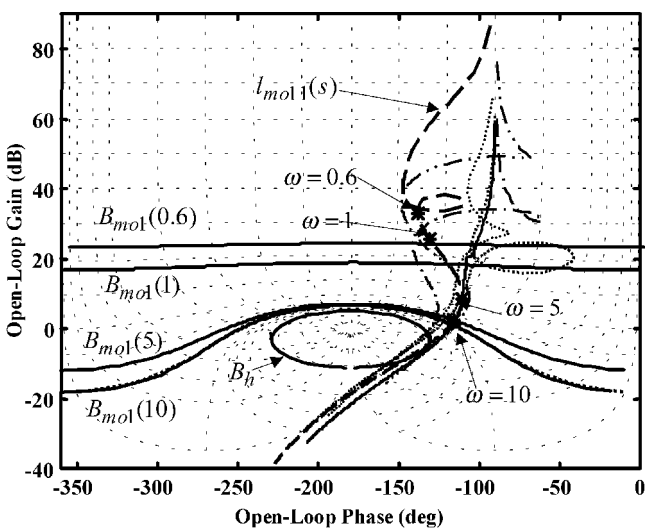

Fig. 4a Channel 1, bounds and loop transmissions of six flight conditions on the inverse Nichols chart.

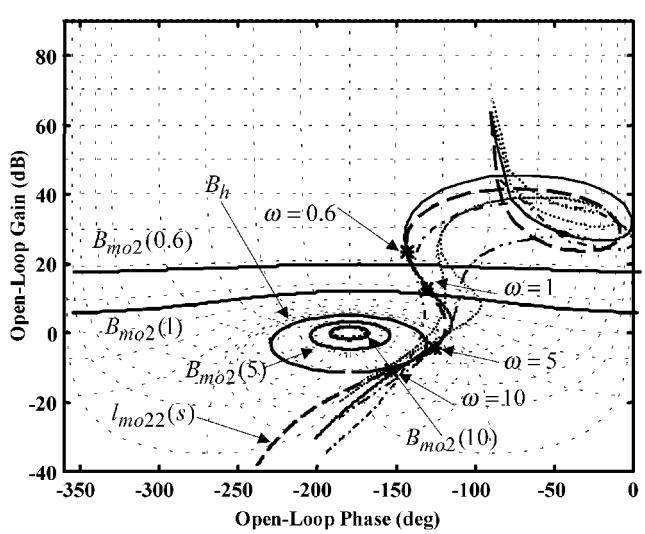

Fig. 4b Channel 2, bounds and loop transmissions of six flight conditions on the inverse Nichols chart.

$$f_{11}(s) = 14/[(s+2)(s+7)] \tag{35}$$

Similarly, for channel 2, B_{2l} and B_{2u} are chosen as nominal and perturbed system responses, as shown in Fig. 3b. Also, the process and the values of bounds are shown in Table 4 and Fig. 4b. The nominal-loop transmission function is chosen as

$$l_{mo22}(s) = \frac{1800(s+0.2)(s+0.5)}{s(s^2+0.0415s+0.1936)(s^2+28.28s+400)} \tag{36}$$

then the required controller $g_{22}(s)$ is obtained as

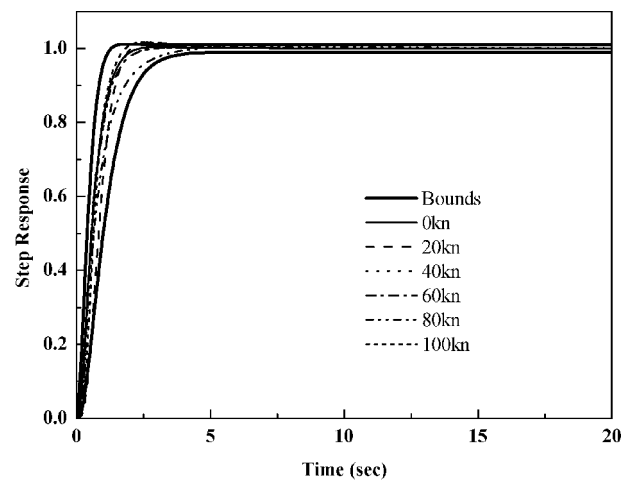

Fig. 5a Closed-loop time responses to step command input $\dot{h}_c = 1$ ft/s: $\dot{h}$ responses for six flight conditions.

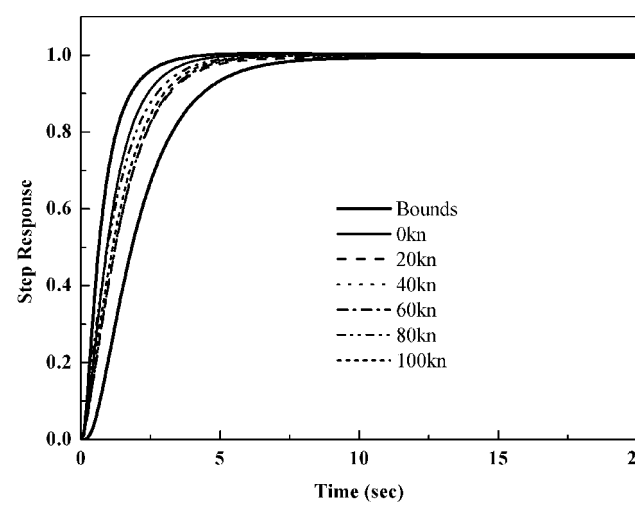

Fig. 5b Closed-loop time responses to step command input $\theta_c = 1$ rad: θ responses for six flight conditions.

$$g_{22}(s) = \frac{-1800(s+0.2)(s+0.45)(s+0.5)(s+3.69)}{s(s+0.0077)(s+0.46)(s^2+28.28s+400)} \tag{37}$$

By the use of simple shaping, the prefilter is obtained as

$$f_{22}(s) = \frac{4.2(s+3.5)}{(s+1)(s+1.4)(s+10.5)} \tag{38}$$

For Fig. 1, by applying the 2-DOF compensators $\boldsymbol{F} = \text{diag}[f_{11}, f_{22}]$ and $\boldsymbol{G} = \text{diag}[g_{11}, g_{22}]$ to the system for different flight conditions, the closed-loop frequency responses are shown in Fig. 3, the loop transmission functions are shown in Fig. 4, and the time-domain simulations are shown in Fig. 5, which shows that the design

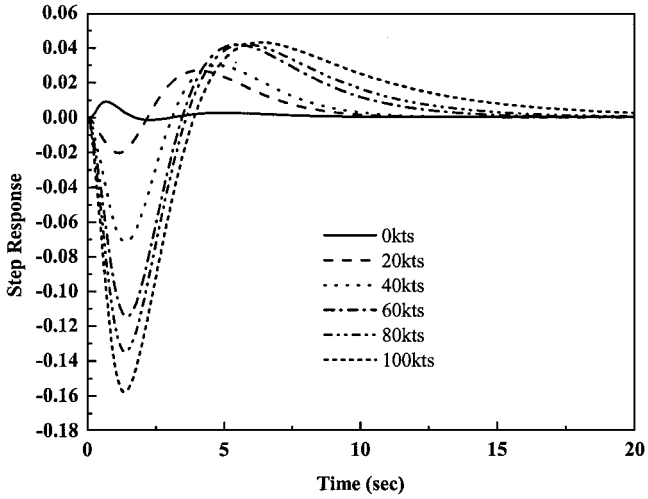

Fig. 5c Coupling time responses to step command input θ_c = 1 rad: $\dot{h}$ (ft/s) responses for six flight conditions.

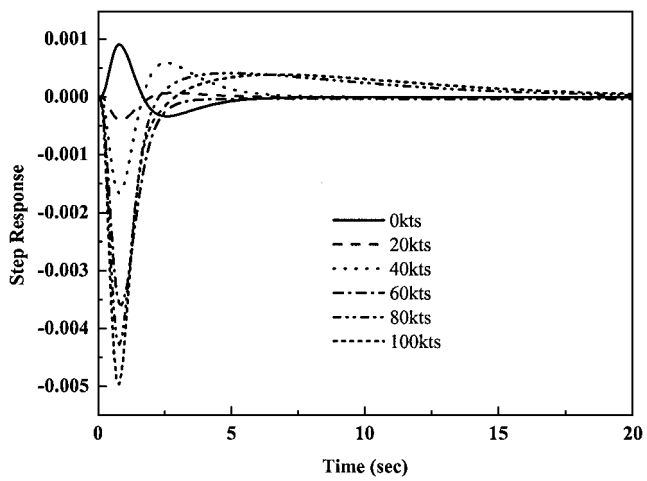

Fig. 5d Coupling time responses to step command input $\dot{h}_c$ = 1 (ft/s): θ (rad) responses for six flight conditions.

performance is achieved. The same example has been presented in Ref. 11 with traditional QFT design method. When the design results are compared, it can be seen that the proposed design method can achieve better performance by assigning a tighter performance bounds and that the proposed design procedure is easier than the traditional QFT because it can obviate the computational workload of creating templates.

IV. Conclusions

An equivalent external disturbance rejection design method for uncertain multivariable systems is developed that can obviate the computational workload of creating templates that must be drawn on Nichols charts in traditional QFT design methodologies. The proposed design method can cope with stable or unstable, minimum-phase or NMP systems, so that it is applied for the longitudinal flight control of a rotorcraft. The design results show that, for all flight conditions, at least 46-deg phase margin is achieved and that the performance bounds are satisfied with the coupling term less than 0.16. This illustrates the robust performance of the proposed design method.

Acknowledgments

This work was supported by the National Science Council of the Republic of China under Grant NSC 89-2213-E-155-041. The authors are grateful to the reviewers and to the Associate Editor for their valuable comments.

References

[1]Horowitz, I. M., and Sidi, M., "Synthesis of Feedback Systems with Large Plant Ignorance for Prescribed Time Domain Tolerance," *International Journal of Control*, Vol. 16, No. 2, 1972, pp. 287–309.

[2]Horowitz, I. M., and Sidi, M., "Optimum Synthesis of Non-Minimum Phase Feedback System with Plant Uncertainty," *International Journal of Control*, Vol. 27, No. 3, 1978, pp. 361–386.

[3]Horowitz, I. M., and Liao, Y. K., "Limitation of Non-Minimum Phase System," *International Journal of Control*, Vol. 40, No. 5, 1984, pp. 1003–1013.

[4]Lin, C. M., and Shi, Z. R., "Quantitative Performance Robustness Linear Quadratic Optimal System Design," *Journal of Guidance, Control, and Dynamics*, Vol. 19, No. 3, 1996, pp. 600–604.

[5]Horowitz, I. M., "Quantitative Synthesis of Uncertain Multiple-Input–Output Feedback System," *International Journal of Control*, Vol. 30, No. 1, 1979, pp. 81–106.

[6]Horowitz, I. M., "Improved Design Technique for Uncertain Multiple Input–Output Feedback Systems," *International Journal of Control*, Vol. 36, No. 6, 1982, pp. 977–988.

[7]Yaniv, O., and Horowitz, I. M., "A Quantitative Design Method for MIMO Feedback Systems Having Uncertain Plants," *International Journal of Control*, Vol. 43, No. 2, 1986, pp. 401–421.

[8]Horowitz, I. M., "Survey of Quantitative Feedback Theory," *International Journal of Control*, Vol. 53, No. 2, 1991, pp. 255–291.

[9]Houpis, C. H., Sating, R. R., Rasmussen, S., and Sheldon, S., "Quantitative Feedback Theory Technique and Application," *International Journal of Control*, Vol. 59, No. 1, 1994, pp. 39–70.

[10]Hess, R. A., and Gorder, P. J., "Quantitative Feedback Theory Applied to the Design of a Rotorcraft Flight Control System," *Journal of Guidance, Control, and Dynamics*, Vol. 16, No. 4, 1993, pp. 748–753.

[11]Hess, R. A., "Rotorcraft Control System Design for Uncertain Vehicle Dynamics Using Quantitative Feedback Theory," *Journal of the American Helicopter Society*, Vol. 39, No. 2, 1994, pp. 47–55.

[12]Gorder, P. J., and Hess, R. A., "Sequential Loop Closure in Design of a Robust Rotorcraft Flight Control System," *Journal of Guidance, Control, and Dynamics*, Vol. 20, No. 6, 1997, pp. 1235–1240.

[13]Chien, C. M., and Wang, B. C., "An SISO Uncertain System Designed by an Equivalent Disturbance Attenuation Method," *Control Theory and Advanced Technology*, Vol. 6, No. 4, 1990, pp. 257–271.

[14]Chien, C. M., and Wang, B. C., "Design Technique for a SISO System with Uncertain Nonminimum-Phase Plant," *IEE Proceedings, Control Theory and Applications*, Vol. 137, No. 6, 1990, pp. 381–384.

[15]Sobhani, M., and Jayasuriya, S., "Control Design for the Size of a Step Disturbance in Non-Minimum Phase, Unstable Uncertain Systems," *International Journal of Control*, Vol. 59, No. 2, 1994, pp. 561–581.

[16]Chien, C. M., Wang, B. C., and Horowitz, I. M., "An Alternative Method for Design of MIMO System with Large Plant Uncertainty," *Control Theory and Advanced Technology*, Vol. 9, No. 4, 1993, pp. 955–969.

[17]Heffley, R. K., "A Compilation and Analysis of Helicopter Handling Qualities Data Vol. 2: Data Analysis," NASA CR-3145, 1979.